

Cite this: *Soft Matter*, 2012, **8**, 11318

www.rsc.org/softmatter

PAPER

Spontaneous pattern formation based on the coffee-ring effect for organic–inorganic hybrid films prepared by dip-coating: effects of temperature during deposition†

Hiroaki Uchiyama,* Daisuke Shimaoka and Hiromitsu Kozuka

Received 8th June 2012, Accepted 31st August 2012

DOI: 10.1039/c2sm26328a

We prepared silica–poly(vinylpyrrolidone) (PVP) hybrid films *via* a temperature-controlled dip-coating process and investigated the influence of the coating temperature (*i.e.*, the temperature of substrates, solutions and atmosphere) on the spontaneous pattern formation based on the “coffee-ring effect”. Micron-scale stripe patterns were spontaneously formed on the surface of the films at high coating temperatures over 40 °C during dip-coating. The stripe patterns were arranged perpendicular to the withdrawal direction, and the height and width of the patterns increased with increasing coating temperature. Such spontaneous pattern formation is attributed to the evaporation-driven capillary flow of coating solutions at the meniscus, and the stripe patterns with larger heights and widths are thought to be achieved by the capillary flow activated at higher coating temperatures.

1. Introduction

Solvent evaporation from solutions containing nonvolatile solutes (*e.g.*, colloidal solutions, suspensions and polymer solutions) often triggers the self-assembly and self-organization of the solutes into complex, ordered micro- and nanostructures. The “coffee-ring effect” is widely known as a typical evaporation-driven self-assembly and self-organization.^{1–12} When a droplet of solutions containing nonvolatile solutes (*e.g.*, coffee) dries on a substrate, it leaves a dense, ring-like deposit of the solutes, *i.e.*, a “coffee ring”, along the perimeter. The evaporative loss of the solvent at the perimeter provides the outward capillary flow of the solutions, resulting in the formation of a “coffee ring” on the substrate. Such pattern formation based on the “coffee-ring effect” can be also found in many coating processes for preparing thin films. In the case of the dip-coating process, where the substrate is dipped into the coating solution and then vertically withdrawn at constant speeds, the pattern formation induced by the capillary flow of coating solutions occurs at the edge of the meniscus during the dip-coating, leading to the formation of stripe patterns arranged perpendicular to the withdrawal direction. The spontaneous formation of arranged stripe patterns during dip-coating has been reported in several types of solutions such as suspensions of nanoparticles^{13,14} and nanowires,^{15–17} colloidal solutions^{18,19} and polymer solutions,^{20,21}

and are expected to be a novel fabrication process of highly ordered patterns in thin films.

Sol–gel coating processes are widely used for preparing inorganic and organic–inorganic hybrid films, where micrometer-sized patterns such as unevenness in thickness or ridges are formed on the surface of the films under certain conditions.^{22–31} We previously prepared sol–gel-derived silica and titania dip-coating films at extremely low substrate withdrawal speeds below 1.0 cm min^{−1}, and found the spontaneous formation of stripe patterns based on the “coffee-ring effect” during the dip-coating.²⁹ The stripe patterns were arranged perpendicular to the withdrawal direction, and the height and width increased with decreasing withdrawal speeds. Such arranged stripe patterns on sol–gel coating films hold great promise for the application in photonic devices such as diffraction gratings and microlens arrays, while it is difficult to precisely control the size and shape of the patterns because of the irregularity in solvent evaporation and in the resultant capillary flow of the solutions. Thus, it is highly desirable to achieve surface patterns with a well-controlled size and shape.

The spontaneous pattern formation induced by the capillary flow of solutions triggered by the solvent evaporation would be significantly influenced by the coating temperature, *i.e.*, the temperature of substrates, solutions and atmosphere. Higher coating temperature increases the evaporation rate of the solvents, promoting the pattern formation induced by the capillary flow. However, the effect of the coating temperature on the “coffee-ring effect” in the dip-coating process has been not fully discussed, which allows us, on the other hand, to control the size of the surface patterns. In this work, we prepared silica–poly(vinylpyrrolidone) (PVP) hybrid films from tetramethyl

Department of Chemistry and Materials Engineering, Kansai University, 3-3-35 Yamate-cho, Suita, 564-8680, Japan. E-mail: h_uchi@kansai-u.ac.jp; Fax: +81-6-6388-8797; Tel: +81-6-6368-1121 extn 5638

† Electronic supplementary information (ESI) available. See DOI: 10.1039/c2sm26328a

orthosilicate (TMOS) solutions containing PVP *via* a temperature-controlled dip-coating process, and investigated the influence of the coating temperature on the spontaneous pattern formation induced by the capillary flow. Dip-coating was performed in a thermostatic oven where the coating temperature, *i.e.*, the temperature of substrates, solutions and atmosphere, was controlled and kept constant. Here, the height and width of the surface patterns were quantitatively evaluated by optical microscopy and surface roughness measurement, and the influence of the coating temperature on the pattern formation based on the “coffee-ring effect” during dip-coating was systematically discussed.

2. Experimental

2.1. Materials

The starting materials were tetramethyl orthosilicate ($\text{Si}(\text{OCH}_3)_4$, TMOS) (Shin-Etsu Silicones, Tokyo, Japan), nitric acid (69 mass%, Wako Pure Chemical Industries, Osaka, Japan), 2-methoxyethanol ($\text{CH}_3\text{OCH}_2\text{CH}_2\text{OH}$) (Wako Pure Chemical Industries), and poly(vinylpyrrolidone) (PVP) (K90, 6.3×10^5 in viscosity average molecular weight, Tokyo Kasei Kogyo Co., Tokyo, Japan).

2.2. Preparation of silica–PVP hybrid films

The compositions of the starting solutions are listed in Table 1. Starting solutions of molar compositions, $\text{TMOS} : \text{H}_2\text{O} : \text{HNO}_3 : \text{CH}_3\text{OCH}_2\text{CH}_2\text{OH} : \text{PVP} = 1 : 2 : 0.01 : 14.8 : x$ ($x = 0$ or 0.5), were prepared by the following procedure, where the mole ratio for PVP was defined for the monomer (polymerizing unit). First, PVP was dissolved in a 3/4 of the prescribed amount of $\text{CH}_3\text{OCH}_2\text{CH}_2\text{OH}$, and then TMOS was added. The remaining amount of $\text{CH}_3\text{OCH}_2\text{CH}_2\text{OH}$ was added to purified water, and then nitric acid was added. The solution containing $\text{CH}_3\text{OCH}_2\text{CH}_2\text{OH}$, purified water and nitric acid was added dropwise to the TMOS solution under stirring. The solutions were allowed to stand at room temperature in a sealed glass container for 30 min, and served as coating solutions.

Hereafter, the TMOS solutions of $x = 0$ and 0.5 are denoted as Solutions P0 and P0.5, respectively. Gel films prepared from the solutions P0 and P0.5 are denoted as Films P0 and P0.5, respectively. Gel films were deposited on a Si(100) substrate ($20 \text{ mm} \times 40 \text{ mm} \times 0.85 \text{ mm}$) using a dip-coater (PORTABLE DIP COATER DT-0001, SDI, Kyoto, Japan), where the substrates were withdrawn at 0.05 cm min^{-1} . The dip-coating was performed in a thermostatic oven as shown in Fig. 1a. The coating temperature, *i.e.*, the temperature of substrates, solutions and atmosphere, was maintained in the range of $25\text{--}70^\circ\text{C}$, where the solutions and substrates were heated at the prescribed

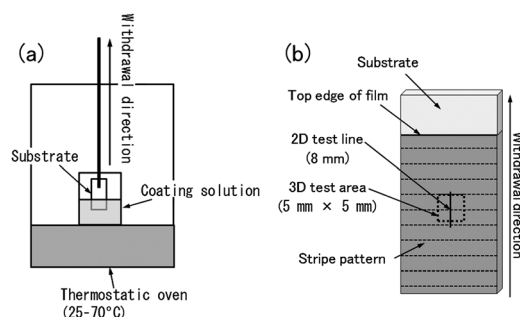


Fig. 1 Schematic illustration of the temperature-controlled dip-coating (a) and the test line and area employed in 2D and 3D surface roughness measurements, respectively (b).

temperature for 30 min before the dip-coating. After the deposition, the thin films were kept at room temperature for 24 h in the ambient atmosphere.

2.3. Characterizations

The viscosity of the coating solutions was measured using an oscillating-type viscometer (VM-1G, Yamaichi Electronics, Tokyo, Japan) in a thermostatic oven, where the temperature of coating solutions was controlled and maintained in the range of $25\text{--}70^\circ\text{C}$. Microscopic observation was made on the films using an optical microscope (KH-1300, HIROX, Tokyo, Japan).

Two- (2D) and three-dimensional (3D) surface profiles of the thin films were measured using a contact probe surface profilometer (SE-3500K31, Kosaka Laboratory, Tokyo, Japan). The measurement was conducted at the center of the thin films as shown in Fig. 1b. Surface roughness parameters, R_z (ten point height of irregularities) and S (mean spacing of local peaks) were calculated from the 2D profile (the definitions of R_z and S are shown in the ESI, Fig. S1†). R_z and S represent the height and spacing, respectively, of the surface patterns. The film thickness was measured by a profilometer (the definitions of the thickness are shown in the ESI, Fig. S1†). A part of the thin film was scraped off with a surgical knife immediately after the film deposition, and the level difference between the coated part and the scraped part was measured after drying. The thickness, R_z and S were measured on three thin film samples, and evaluated three times per one sample. And then, the averages and standard deviations were calculated from the nine values.

3. Results and discussion

3.1. Surface patterns of silica–PVP hybrid films

Coating solutions without and with PVP (Solutions P0 and P0.5) were prepared at room temperature. The viscosity of the

Table 1 Compositions and viscosity of the coating solutions

Solutions	Mole ratio					Viscosity $\text{mPa}^{-1} \text{s}^{-1}$
	TMOS	H_2O	HNO_3	$\text{CH}_3\text{OCH}_2\text{CH}_2\text{OH}$	PVP (x)	
P0	1	2	0.01	14.8	0	2.29
P0.5	1	2	0.01	14.8	0.5	39.5

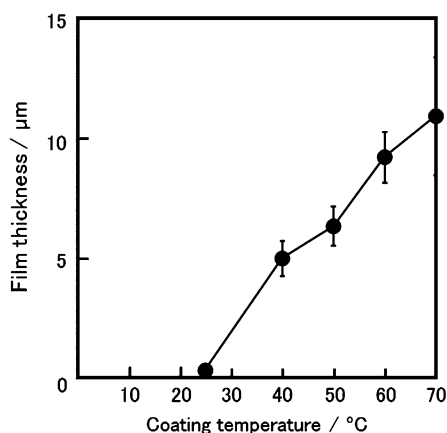


Fig. 2 Dependence of film thickness on coating temperature for the silica-PVP hybrid films (Films P0.5). Error bars indicate the standard deviations.

solutions increased with the addition of PVP as shown in Table 1, which was almost unchanged at temperatures ranging from 25 to 70 °C (ESI, Fig. S2†).

Silica and silica-PVP hybrid films (Films P0 and P0.5) were prepared from Solutions P0 and P0.5, respectively, where the coating temperature was changed between 25 and 70 °C. Cracked gel films were obtained from Solution P0 irrespective of the coating temperature (Films P0). On the other hand, cracks were not observed for Films P0.5 under all conditions. Addition of PVP suppresses the stress evolution attributed to the condensation reaction of metaloxane polymers in gel films, and consequently allows thick coatings to be formed without cracking.³²

Fig. 2 shows the dependence of the thickness on the coating temperature for crack-free Film P0.5. The film thickness increased with increasing coating temperature. This could be explained as follows in terms of capillary flow triggered by the

solvent evaporation. During the dip-coating of extremely low substrate withdrawal speeds below 0.01 mm s^{-1} (0.06 cm min^{-1}), the solvents evaporate from the edge of the meniscus, and then the coating solution is raised to the edge of the meniscus by a capillary force.^{33,34} As a result of the upward capillary flow, the edge of the coating solution is pinned to the substrate, and thus the downward flow of the solution by gravity is suppressed, leading to an increase in the film thickness. Such pining phenomenon of solutions induced by capillary flow is commonly known as the “coffee-ring effect”.^{2,3} In the present case, higher coating temperatures could promote the capillary flow of coating solution, resulting in larger thickness.

A typical dip-coating film prepared at extremely low substrate withdrawal speeds is shown in Fig. 3a, where stripe patterns arranged perpendicular to the substrate withdrawal direction are visually confirmed on the surface. In this work, such surface patterns were visually detected for Films P0.5 prepared over 40 °C. Fig. 3b–f show the optical micrographs of Films P0.5 prepared in the range of 25–70 °C. A smooth surface with inhomogeneity in interference color was obtained at 25 °C (Fig. 3b). On the other hand, stripe patterns of 300–500 μm in spacing arranged perpendicular to the withdrawal direction were formed over 40 °C, and the patterns became clear with increasing coating temperature (Fig. 3c–f). Fig. 4 shows the 3D surface profiles of Films P0.5 prepared at 25, 40 and 60 °C. Specific patterns were not observed for Films P0.5 prepared at 25 °C (Fig. 4a). Stripe patterns of 3.0–6.0 μm height and 300–500 μm width were found on those prepared over 40 °C (Fig. 4b and c). The height and width of the stripe patterns increased with increasing coating temperature as seen in the profiles.

Fig. 5 shows the dependence of the roughness parameters, R_z and S , on the coating temperature for Film P0.5. It is clear from the 3D surface profiles (Fig. 4) that R_z and S values for the samples prepared over 40 °C correspond to the height and spacing of the stripe patterns, respectively, while those at 25 °C

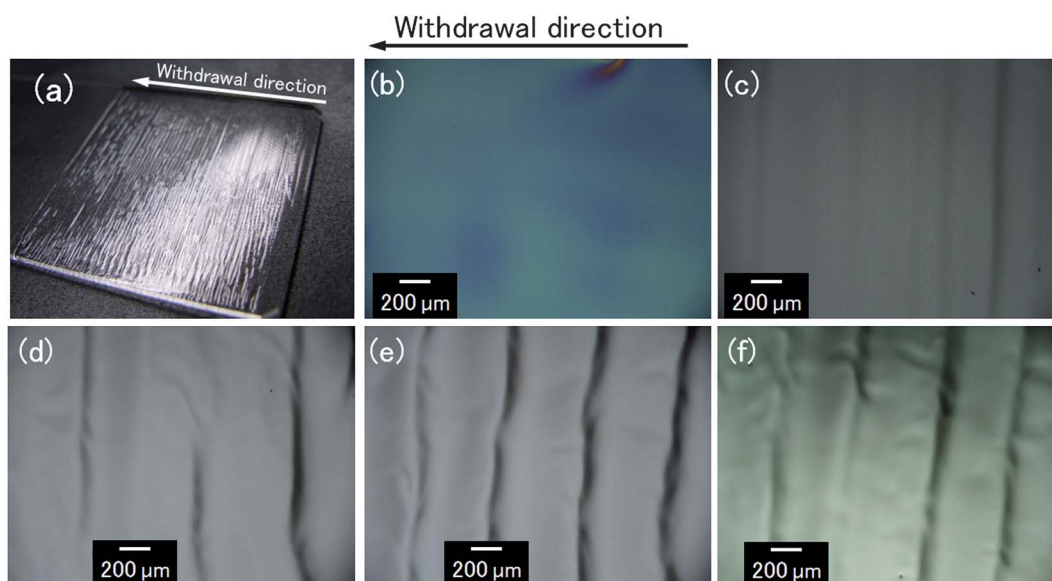


Fig. 3 A typical dip-coating film prepared at the extremely low substrate withdrawal speeds (a), and optical micrographs of the silica-PVP hybrid films (Films P0.5) prepared at 25 (b), 40 (c), 50 (d), 60 (e) and 70 °C (f).

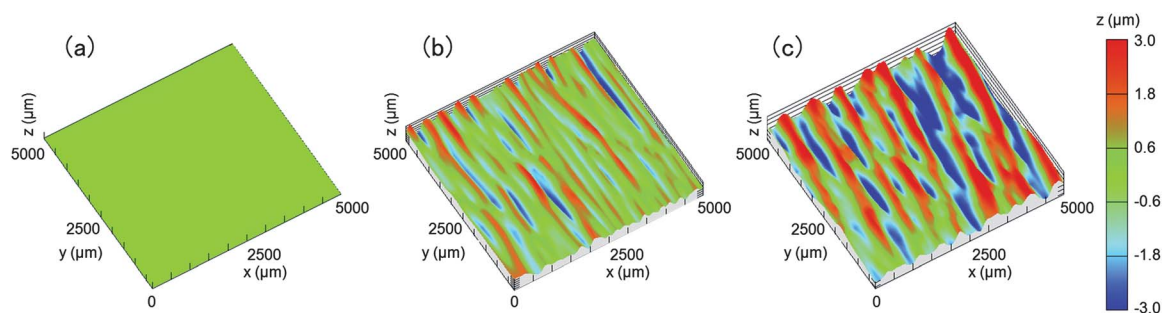


Fig. 4 3D surface profiles of the silica–PVP hybrid films (Films P0.5) prepared at 25 (a), 40 (b) and 60 °C (c).

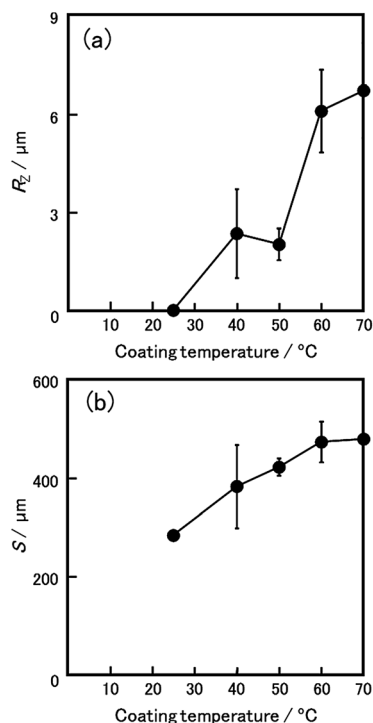


Fig. 5 Dependence of R_z (a) and S (b) on coating temperature for the silica–PVP hybrid films (Films P0.5). Error bars indicate the standard deviations.

are rather attributed to the intrinsic surface roughness, not to stripe patterns. The increase in the coating temperature led to an increase in R_z and S , *i.e.* in height and spacing of the stripe patterns, which agreed with the 3D profiles shown in Fig. 4.

3.2. The mechanism of spontaneous formation of stripe patterns at an extremely low withdrawal speed

Stripe patterns arranged perpendicular to the withdrawal direction were formed on the surface of silica–PVP hybrid dip-coating films prepared at an extremely low substrate withdrawal speed (0.05 cm min^{-1}) (Fig. 3 and 4), which could be attributed to the capillary flow of coating solution at the edge of the meniscus. As mentioned in the Section 3.1, during the dip-coating at such low substrate withdrawal speeds, the edge of the coating solution is pinned to the substrate by the evaporation-driven capillary flow. Such pinning phenomenon due to the capillary flow often leads

to the formation of periodic patterns through the repetition of the pinning of viscous solutions at their edge, which is called “stick-slip motion”.^{4,7,13–21,29} The schematic illustration of the pattern formation induced by “stick-slip motion” in sol–gel films is shown in Fig. 6. Firstly, the gelation of the coating solution locally progresses at the edge of the meniscus due to the solvent evaporation. And then, the coating solution is continuously supplied to the edge of the meniscus by the capillary flow during solvent evaporation. Consequently, the thickness of the coating layer locally increases at the edge of the meniscus, leading to the formation of a convex gel part. The convex part is continuously raised with the substrate withdrawal, and progressively segregated from the meniscus. As a result, the edge of the coating solution moves downward like a receding tide until the next pinning occurs by the capillary flow. Stripe patterns arranged perpendicular to the withdrawal direction could thus be formed through the repetition of the pinning of coating solution at their edge and the formation of convex gel part there.

The formation of stripe patterns was observed over 40 °C (Fig. 3 and 4), and the increase in the coating temperature led to the increase in the height and width of the patterns (Fig. 5). The rapid solvent evaporation at higher coating temperatures is thought to activate the capillary flow of the coating solution towards the edge of meniscus, resulting in the increase in the height and width of the patterns.

The effect of temperature on the pattern formation induced by “stick-slip motion” was previously investigated for products obtained from suspensions of nanoparticles and colloidal solutions.^{13,14} Olgun *et al.* demonstrated the formation of stripe patterns of zeolite nanoparticles on glass substrates, where the increase in temperature resulted in the increase in the width of stripes.¹³ Watanabe *et al.* investigated the mechanism of stripe pattern formation on hydrophilic surfaces using suspensions of

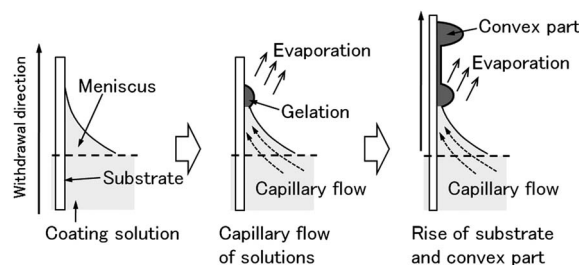


Fig. 6 Schematic illustration of the pattern formation induced by stick-slip motion.

silica spheres, and reported that the width and spacing of the stripes are almost constant regardless of the solvent evaporation rate.¹⁴ In those cases, the size of stripe patterns is determined by the equilibrium between the growth of the convex part and the downward movement of the edge of solutions, which is also the case with the sol–gel-derived silica–PVP films.

On the other hand, in the case of the sol–gel processes, the hydrolysis and condensation reactions of alkoxides result in the increase in solution viscosity, leading to gelation. The hydrolysis and condensation rates increase with increasing temperature. Thus, in the present work, the increase in the size of the patterns at higher temperatures might be also attributed to the increase in the growth rate of the convex gel part due to the higher hydrolysis and condensation rates.

In the present work, a smooth surface without specific surface patterns was observed for Films P0.5 prepared at 25 °C (Fig. 3b). On the other hand, in our previous work, we prepared silica– and titania–PVP films by dip-coating in the ambient atmosphere (ca. 25 °C), where stripe patterns attributed to “stick-slip motion” were found on the surface of the films at 0.02–0.3 cm min⁻¹.²⁹ The difference in the pattern formation could be attributed to the boiling point of the solvents of coating solutions. In the previous and present works, C₂H₅OH (boiling point: 78.3 °C) and CH₃OCH₂CH₂OH (boiling point: 125 °C) were used as the solvents, respectively. The slower evaporation of CH₃OCH₂CH₂OH suppressed the capillary flow of coating solution during the dip-coating, resulting in the formation of smooth surface.

4. Conclusion

We investigated the influence of coating temperature on the spontaneous pattern formation based on the “coffee-ring effect” for sol–gel-derived silica–PVP hybrid films. Silica–PVP hybrid films were prepared at an extremely low substrate withdrawal speed (0.05 cm min⁻¹) via the temperature-controlled dip-coating process, where micron-scale stripe patterns arranged perpendicular to the withdrawal direction were spontaneously formed with increasing coating temperature. Such periodic surface patterns were thought to form through the evaporation-driven capillary flow of coating solution to the edge of the meniscus and the formation of convex parts due to the gelation there. The height and width of stripe patterns increased with increasing coating temperature. Higher coating temperature promoted the capillary flow of coating solution, leading to the formation of stripe patterns with larger heights and widths. Such an evaporation-driven self-organization process would be useful for the fabrication process of highly ordered patterns in inorganic and organic–inorganic thin films.

References

- 1 S. Choi, S. Stassi, A. P. Pisano and T. I. Zohdi, *Langmuir*, 2010, **26**, 11690–11698.
- 2 R. D. Deegan, O. Bakajin, T. F. Dupont, G. Huber, S. R. Nagel and T. A. Witten, *Nature*, 1997, **389**, 827–829.
- 3 R. D. Deegan, O. Bakajin, T. F. Dupont, G. Huber, S. R. Nagel and T. A. Witten, *Phys. Rev. E: Stat. Phys., Plasmas, Fluids, Relat. Interdiscip. Top.*, 2000, **62**, 756–765.
- 4 W. Han and Z. Q. Lin, *Angew. Chem., Int. Ed.*, 2012, **51**, 1534–1546.
- 5 P. Innocenzi, L. Malfatti, M. Piccinini, D. Grosso and A. Marcelli, *Anal. Chem.*, 2009, **81**, 551–556.
- 6 D. Kim, S. Jeong, B. K. Park and J. Moon, *Appl. Phys. Lett.*, 2006, **89**, 264101.
- 7 J. Xu, J. F. Xia and Z. Q. Lin, *Angew. Chem., Int. Ed.*, 2007, **46**, 1860–1863.
- 8 T. Still, P. J. Yunker and A. G. Yodh, *Langmuir*, 2012, **28**, 4984–4988.
- 9 H. Hu and R. G. Larson, *J. Phys. Chem. B*, 2006, **110**, 7090–7094.
- 10 H. M. Ma, R. Dong, J. D. Van Horn and J. C. Hao, *Chem. Commun.*, 2011, **47**, 2047–2049.
- 11 W. D. Ristenpart, P. G. Kim, C. Domingues, J. Wan and H. A. Stone, *Phys. Rev. Lett.*, 2007, **99**, 234502.
- 12 M. Yoldi, C. Arcos, B. R. Paulke, R. Sirera, W. González-Viñas and E. Görnitz, *Mater. Sci. Eng., C*, 2008, **28**, 1038–1043.
- 13 U. Olgun and V. Sevinc, *Powder Technol.*, 2008, **183**, 207–212.
- 14 S. Watanabe, K. Inukai, S. Mizuta and M. T. Miyahara, *Langmuir*, 2009, **25**, 7287–7295.
- 15 J. X. Huang, R. Fan, S. Connor and P. D. Yang, *Angew. Chem., Int. Ed.*, 2007, **46**, 2414–2417.
- 16 N. L. Liu, Y. Zhou, L. Wang, J. B. Peng, J. A. Wang, J. A. Pei and Y. Cao, *Langmuir*, 2009, **25**, 665–671.
- 17 C. Y. Zhang, X. J. Zhang, X. H. Zhang, X. Fan, J. S. Jie, J. C. Chang, C. S. Lee, W. J. Zhang and S. T. Lee, *Adv. Mater.*, 2008, **20**, 1716–1720.
- 18 H. Bodiguel, F. Doumenc and B. Guerrier, *Langmuir*, 2010, **26**, 10758–10763.
- 19 M. Ghosh, F. Q. Fan and K. J. Stebe, *Langmuir*, 2007, **23**, 2180–2183.
- 20 J. Jang, S. Nam, K. Im, J. Hur, S. N. Cha, J. Kim, H. B. Son, H. Suh, M. A. Loth, J. E. Anthony, J. J. Park, C. E. Park, J. M. Kim and K. Kim, *Adv. Funct. Mater.*, 2012, **22**, 1005–1014.
- 21 G. Pu and S. J. Severtson, *Langmuir*, 2008, **24**, 4685–4692.
- 22 D. P. Birnie, *J. Mater. Res.*, 2001, **16**, 1145–1154.
- 23 D. P. Birnie, D. M. Kaz and D. J. Taylor, *J. Sol-Gel Sci. Technol.*, 2009, **49**, 233–237.
- 24 D. E. Haas and D. P. Birnie, *J. Mater. Sci.*, 2002, **37**, 2109–2116.
- 25 H. Kozuka, *J. Ceram. Soc. Jpn.*, 2003, **111**, 624–632.
- 26 H. Kozuka and M. Hirano, *J. Sol-Gel Sci. Technol.*, 2000, **19**, 501–504.
- 27 H. Kozuka, Y. Ishikawa and N. Ashibe, *J. Sol-Gel Sci. Technol.*, 2004, **31**, 245–248.
- 28 S. Shibata, K. Miyajima, H. Yoshikawa, T. Yano and M. Yamane, *J. Sol-Gel Sci. Technol.*, 2000, **19**, 665–669.
- 29 H. Uchiyama, M. Hayashi and H. Kozuka, *RSC Adv.*, 2012, **2**, 467–473.
- 30 H. Uchiyama, Y. Miki, Y. Mantani and H. Kozuka, *J. Phys. Chem. C*, 2012, **116**, 939–946.
- 31 H. Uchiyama, W. Namba and H. Kozuka, *Langmuir*, 2010, **26**, 11479–11484.
- 32 H. Kozuka, *J. Sol-Gel Sci. Technol.*, 2006, **40**, 287–297.
- 33 M. Faustini, B. Louis, P. A. Albouy, M. Kuemmel and D. Grosso, *J. Phys. Chem. C*, 2010, **114**, 7637–7645.
- 34 D. Grosso, *J. Mater. Chem.*, 2011, **21**, 17033–17038.